Discretization of Tilted FBGs Spectra for Sensing and Coding

Ander Zornoza, Efraín Villatoro, *Member, IEEE*, Plácido Zaca-Morán, Celia L. Gomez, Rubén Ramos-García, Jacques Albert, and Joel Villatoro, *Senior Member, IEEE*

***Abstract*— Tilted fiber Bragg gratings (TFBGs) give rise to a dense comb of cladding mode resonances for which they are appealing for high-resolution sensing. However, the interrogation of such gratings tends to be complex and expensive. As an alternative to conventional interrogation approaches, herein, we propose to discretize the TFBG spectra to form binary codes of "0" and "1" and to correlate such bits with different values of a target measurand. As an example, we demonstrate the measurements of water–alcohol mixtures with TFBGs excited with randomly polarized light and interrogated over a narrow (6 nm) wavelength range. We have found that for each mixture surrounding a TFBG, a unique set of bits can be generated. As bits are the language of digital technologies and are easy to process, we believe that the approach proposed here can pave the way for a new manner of interrogating TFBGs. Moreover, the binary codes generated by discretization of TFBG spectra may allow the generation of unique visual labels (barcodes) for the identification of liquids, thereby expanding the applications of TFBGs.**

***Index Terms*— Optical fiber sensors, refractometry, spectral barcodes, tilted fiber Bragg gratings (TFBG).**

I. Introduction

TILTED fiber Bragg gratings (TFBGs) are a family of gratings that have periods like those of conventional fiber Bragg gratings, but with tilted grating planes relative to the optical fiber axis [1], [2], [3]. Like fiber Bragg gratings, TFBGs are fabricated by exposing a standard single-mode optical fiber to a periodic laser pattern created via free-space interferometry or a diffractive phase mask [4]. Nowadays, the inscription process of conventional and tilted Bragg gratings is well established and mature. This ensures important features for optical sensing as reliable and robust TFBGs can be produced in high volumes.

The inclination angle of the grating planes of a TFBG allows the excitation of multiple cladding modes [5], [6], [7]. Since the cladding diameter of a conventional optical fiber (typically 125 μm) is much larger than the excitation wavelength (around 1.55 μm), tens or hundreds of cladding modes can be excited, each mode at a specific wavelength. The excited cladding modes can be identified as narrowband ($\sim$0.2 nm) resonances in the transmission or reflection spectrum of a TFBG.

The tilt angle, the period, and length of the grating as well as the strength of the refractive-index modulation of the grating and the polarization of the input light allow to control the number and amplitude of cladding mode resonances. All these control parameters make it easy to excite cladding modes in a selective manner. That is why the interest in TFBGs for sensing applications has grown in the last few years [8], [9], [10].

It is well known that cladding modes are sensitive to the environment that surrounds the fiber cladding or to nanolayers deposited on the same. Thus, in the last two decades, TFBGs have been widely used for refractometry [11], [12], [13], [14] and for highly sensitive biochemical sensing [15], [16], [17], [18]. For refractometry, TFBGs feature some advantages. For example, TFBGs can be used without any intermediate nanocoatings and no additional fiber etching or tapering is necessary to interact with liquids. This is of great advantage for refractive index sensing as robustness and reliability are not compromised and the sensor fabrication steps are reduced.

The refractive index value of a substance surrounding a TFBG can be known, for example, by analyzing the upper and lower envelopes of the complete spectral comb [19], [20], [21] or by monitoring the wavelength separation of some cladding mode resonances from the Bragg wavelength [22], [23], [24]. In these cases, an interrogation scheme with high spectral resolution over a wide range (approximately 70 nm) is necessary. However, the most popular approach consists of correlating the wavelength of the cutoff mode resonance

Received 14 June 2024; revised 28 August 2024; accepted 3 September 2024. Date of publication 7 October 2024; date of current version 21 October 2024. This work was supported in part by MCIN/AEI/10.13039/501100011033 under Grant PID2023-152763NB-I00, Grant PID2021-122505OBC31, and Grant TED2021-129959B-C21; in part by the "European Regional Development Fund (ERDF) A Way of Making Europe"; in part by European Union Next Generation European Union (EU)/Plan de Recuperación, Transformación y Resiliencia (PRTR); in part by Grant IT11452-22; in part by ELKARTEK 2023 funded by the Basque Government under Grant μ4Smart-KK-2023/00016 and Grant Ekohegaz II-KK-2023/00051; and in part by the University of the Basque Country (UPV/EHU) Translight. The work of Efraín Villatoro was supported in part by Mexican Consejo Nacional de Humanidades, Ciencias y Tecnologías (CONAHCYT) for a Ph.D. Fellowship. The work of Jacques Albert was supported by NSERC fund RGPIN-2019-06255 and in part by the Canada Research Chairs program. The Associate Editor coordinating the review process was Dr. Ting-Wei Wang. *(Corresponding authors: Joel Villatoro; Ander Zornoza.)*

Ander Zornoza is with the Department of Applied Mathematics, University of the Basque Country UPV/EHU, E-48013 Bilbao, Spain (e-mail: ander.zornoza@ehu.eus).

Efraín Villatoro and Rubén Ramos-García are with the National Institute of Astrophysics, Optics and Electronics (INAOE), 72840 Puebla, Mexico (e-mail: efrain.vip@gmail.com; garcia@inaoep.mx).

Plácido Zaca-Morán and Celia L. Gomez are with the Instituto de Ciencias, Benemérita Universidad Autónoma de Puebla, 72050 Puebla, Mexico (e-mail: placido.zaca@correo.buap.mx; celia.gomez@correo.buap.mx).

Jacques Albert is with the Department of Electronics, Carleton University, Ottawa, ON K1S 5B6, Canada (e-mail: jacquesalbert@cunet.carleton.ca).

Joel Villatoro is with the Department of Communications Engineering, University of the Basque Country UPV/EHU, 48013 Bilbao, Spain, and also with IKERBASQUE, Basque Foundation for Science, 48011 Bilbao, Spain (e-mail: agustinjoel.villatoro@ehu.eus).

Digital Object Identifier 10.1109/TIM.2024.3470969

with the refractive index of the sample [25], [26], [27]. The cutoff mode is identified in the spectral comb as the cladding mode with a reduced transmission amplitude, indicating a transition out of effective guiding conditions. The disadvantage of this approach is the so-called cutoff mode hopping, which leads to a staircase calibration curve [28], [29], [30]. Some research groups have overcome this issue with appropriate signal processing. For example, signal processing based on convolutional neural networks [31], differential spectral responses [32], or the derivative of the envelope of the spectral comb [33] have been reported. However, such signal processing also requires bulky instruments with high spectral resolution.

Despite the advances in signal processing mentioned above, TFBG-based refractometers and other biochemical sensors still have some important disadvantages. These include the need of polarization control, the requirement of monitoring the Bragg wavelength and many cladding mode resonances, or only a specific (cutoff) resonance. Polarization controllers and broadband high-resolution spectral analysis increase the complexity and cost of the interrogation of TFBG-based sensors. In addition, the spectral changes of TFBGs are difficult to interpret; hence, it is not easy to transform such changes into quantitative information about the measurand. All these factors limit the practical applications of TFBG sensors. Therefore, it is important to propose new alternatives to the processing of the spectra generated by TFBGs to allow wider use of sensors based on such gratings.

As an alternative to prior art, in this work, we propose to discretize the TFBG spectral combs to form binary codes of “0” and “1” to represent different values of the surrounding environment. This means we propose to use the well-established language of digital technologies to decode the spectral combs. It will be demonstrated that a unique set of bits and barcodes can be generated from the output spectra of TFBGs immersed in different liquids. We believe that our approach can be useful in applications of TFBG sensors, where the identification of a threshold is the only measurement needed. The main advantage of our approach is that the TFBGs can be interrogated in a narrow spectral range (6 nm) even with low spectral resolution. It is also possible to implement an inexpensive interrogation system for TFBG sensors with a narrowband tunable laser and photodetectors.

In addition to monitoring the refractive index of liquids, TFBGs can be used for coding or labeling. This means our work can expand the use and applications of tilted Bragg gratings.

II. Materials and Methods

The TFBGs used in our experiments were fabricated at the facilities of the Advanced Photonic Components Laboratory at Carleton University, Canada. The gratings were inscribed in a standard single-mode optical fiber, SMF-28 from Corning. To enhance photosensitivity, the optical fiber was loaded with hydrogen for 14 days at a pressure of 17 MPa. After that, the gratings were written by irradiating the optical fiber with a pulsed KrF excimer laser at 248 nm and using a phase mask inclined with respect to the fiber axis [4]. Under these conditions, a permanent change in the refractive index of the fiber core was achieved. Afterward, the TFBGs were baked at 100 °C for 12 h to accelerate the hydrogen diffusion and obtain a stable spectrum. All the TFBGs fabricated and used in our experiments had a tilt angle of 10°; the Bragg wavelength was 1610 nm, and a grating length was 10 mm.

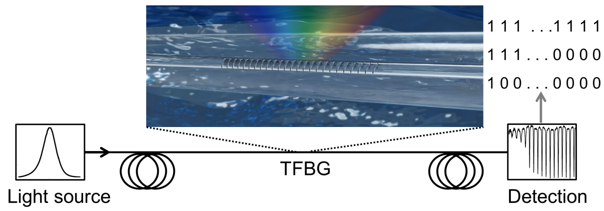

Fig. 1. Schematic of the experimental setup. Data from the detection system are postprocessed to generate the bits.

After the fabrication, we measured the TFBG transmission spectra over a wide wavelength range (full spectrum not shown). To monitor the Bragg wavelength (located at 1610 nm) and all the cladding mode resonances that expanded to 1520 nm, two amplified spontaneous emission light sources (JDSU model BBS1560-2FA and BBS1590-1FA) mixed with a broadband coupler and a 20-pm resolution optical spectrum analyzer (Yenista OSA20) were used. Such characterization setup of the TFBGs is not practical for low-cost sensing applications. Thus, we implemented an interrogation setup, sketched in Fig. 1, with a homemade narrowband (∼20 nm) light source and an optical spectrum analyzer (Anritsu model MS9740A with a resolution of 50 pm at 1550 nm) that was available during the experiments. Polarization controllers were not used. The light source was implemented with a segment of erbium-doped optical fiber pumped with a laser diode (model BL976-SAG300 from Thorlabs), lasing wavelength of 976 nm, and controlled by a stabilized laser diode driver (model LDC250C from Thorlabs). The generated light had a Gaussian spectral shape with peak emission at 1560 nm and full-width at half-maximum (FWHM) of 10 nm. Even though we monitored only a slice of the TFBG spectrum, we could discretize the spectra and correlate the generated binary codes with the refractive index of the liquids that surrounded the TFBG.

The sensing of liquids was implemented as follows. We immersed the TFBG in different mixtures of tri-distilled water and isopropyl alcohol (IPA). To do so, we prepared several sets of 5 mL each, with IPA concentrations ranging from 0% to 100% v/v. After that, we proceeded to immerse the TFBG in different mixtures. During our experiments, the TFBG was carefully secured with a pair of fiber holders to tense the fiber and to eliminate possible wavelength shifts of the comb when the TFBG was immersed in the water–IPA solutions. After immersing the TFBG in each mixture, the zone of the fiber with the grating was cleaned with plenty of water and dried with air. All the experiments were carried out at a room temperature, approximately at 24 °C, with fluctuations of about 2 °C. The experiments were carried out 5 times

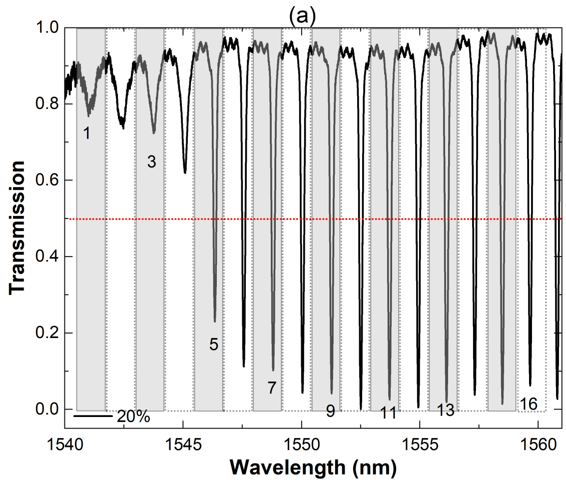

Fig. 2. (a) Transmission spectrum of a TFBG in a mixture of water–IPA with 20% IPA concentration. (b) Spectrum of the same TFBG when the IPA concentration was 50%. The resonances are numbered from 1 to 16. The shadowed and dotted rectangles show the spectral windows, where the absolute minima were calculated. The horizontal dotted lines show an arbitrary threshold.

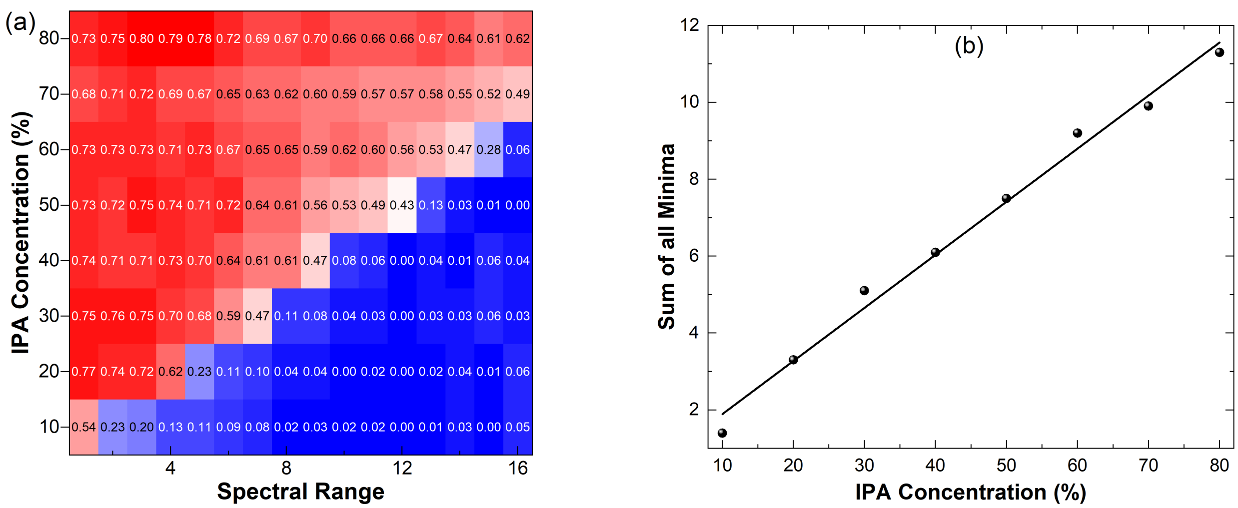

Fig. 3. (a) Minima of the 16 spectral ranges shown in Fig. 2(a) and (b) observed in a TFBG immersed in different water–IPA mixtures. (b) Sum of the 16 minima as a function of IPA concentration.

by increasing and decreasing the IPA concentrations in steps of 10% v/v.

III. Results and Discussion

Fig. 2(a) and (b) shows the normalized transmission spectra of the TFBG described in the above paragraphs when it was immersed in tri-distilled water with two concentrations of isopropyl alcohol. The spectra were normalized to the power spectrum of the light source. The observed resonances in the monitored wavelength range are numbered from 1 to 16. We have chosen 16 resonances because it is a multiple of an 8-bit byte, which is the basic computing unit. It can be noted that resonance 4 in Fig. 2(a), dip at 1545.07 nm, and resonance 12 in Fig. 2(b), dip at 1555.26 nm, are the cutoff modes for the concentration of 20% and 50% v/v, respectively. While the wavelength of the cutoff mode can be used to determine the concentration (i.e., refractive index), this method has limited accuracy because of the wavelength separation between mode resonances [12].

To discretize the spectra, we divided them into 16 spectral ranges, which are highlighted with shaded and dotted rectangles in Fig. 2(a) and (b). Each spectral range had a width of 1.25 nm and had only one resonance. The spectral ranges are wide enough to ignore any small wavelength shifts of the resonances that can be due to temperature drift, small bending, or strain in the optical fiber. The absolute minimum of the 16 spectral ranges for concentrations of IPA between 10% and 80% v/v is shown in Fig. 3(a). All the minima were rounded to two decimal points. In Fig. 3(b), we show the sum of the 16 minima as a function of IPA concentration. The results shown in Fig. 3(b) suggest that it is possible to quantify the changes of the environment that surrounds a TFBG by tracking the minimum of a small number of resonances.

To generate a binary code from the data shown in Fig. 3(a), we established an arbitrary threshold to the calculated minima. As shown in Fig. 2(a) and (b), with horizontal dotted lines, the threshold was set to 0.5 on the normalized transmission

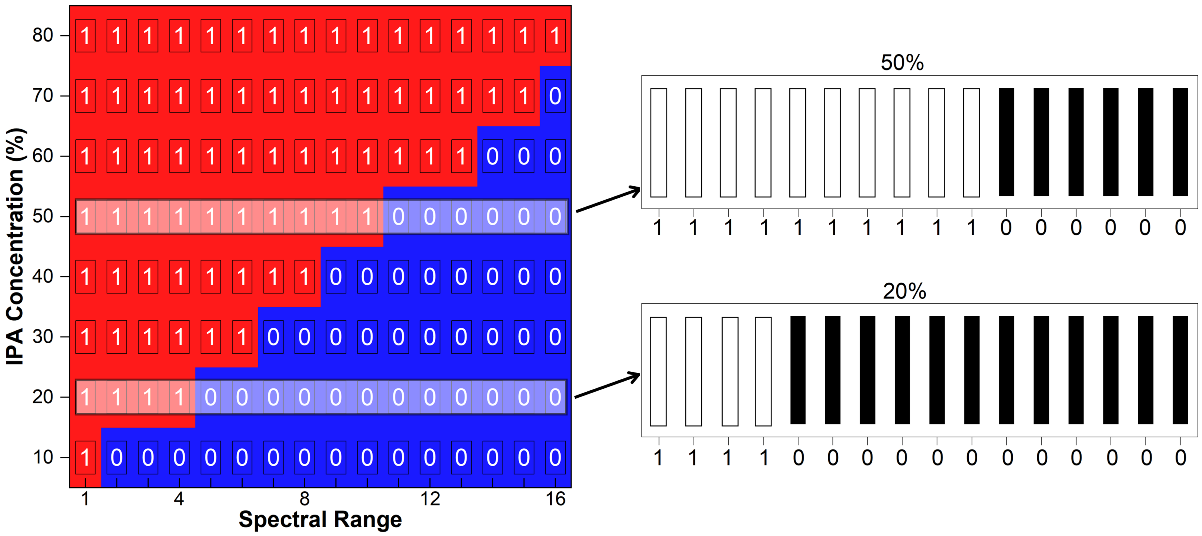

(a) (b)

Fig. 4. (a) Binary codes generated for different IPA concentrations based on the minima of Fig. 3(a) and the arbitrary thresholds (0.5) shown in Fig. 2(a) and (b). Two 1-D barcodes generated with the set of bits, highlighted with the shadowed rectangles, are also shown.

spectrum, although any other value can be chosen. Thus, the minima below 0.5 were considered 0 and 1 for those above 0.5. The resulting binary digits for all the measured concentrations are shown in Fig. 4. It can be observed that each IPA concentration generates a unique set of bits, but in all cases, the information generated by each concentration is only 2 bytes.

One-dimensional barcodes can also be implemented with a series of bits. As an example, in Fig. 4, we show the barcodes generated for an IPA concentration of 20% and 50% v/v. Once a barcode is generated, it can be decoded fast with a simple and inexpensive read out unit. That is why barcodes are widely used in our daily lives; popular applications include labeling and identification of all sorts of items.

The discretization of the TFBG spectra discussed above allows the generation of unique bits or barcodes. The latter can be an alternative to the multicolor optical barcodes generated from the collective behavior of the reflection or transmission spectrum of microresonators [34], [35], [36], lasers [37], or interferometers [38]. In these cases, high spectral resolution over a broad spectral range is required. Moreover, the decoding of multicolor optical barcodes is not straightforward.

The above results were obtained by postprocessing the data collected with a bulky optical spectrum analyzer, which cannot be practical in many applications. Presently, compact, cost-effective low-resolution spectrometers and tunable lasers that operate in a narrowband are commercially available and so are photodiode arrays and demultiplexers. If such alternatives are used to implement an interrogation scheme for TFBGs, the transmitted spectral comb can be monitored. When using low-resolution spectrometers, the measured spectra are also given by the input optical power in the resolution wavelength window given by the spectral resolution. In the case of a demultiplexer and photodetectors, the photodiodes output electric current is given by the input optical power

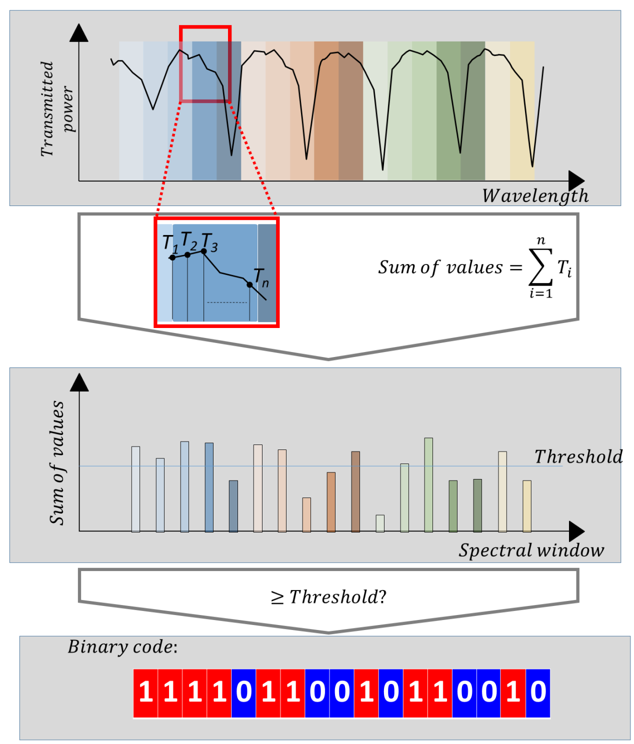

Fig. 5. Schematic of the discretization process. First, the spectra are divided into windows. Second, the sum of values of each window is calculated by the sum of the transmitted powers in that window. Third, the value of the sum of values is compared to a threshold value to obtain the binary code.

in a given wavelength window. To simulate the interrogation of our TFBGs in transmission mode with a narrowband and low-resolution system, we proceeded as depicted in Fig. 5. We analyzed only a small range over the spectra of the TFBG. For each IPA concentration, the monitored spectrum must be divided into a finite number of spectral windows. To mimic the behavior of low-resolution spectrometers or demultiplexer

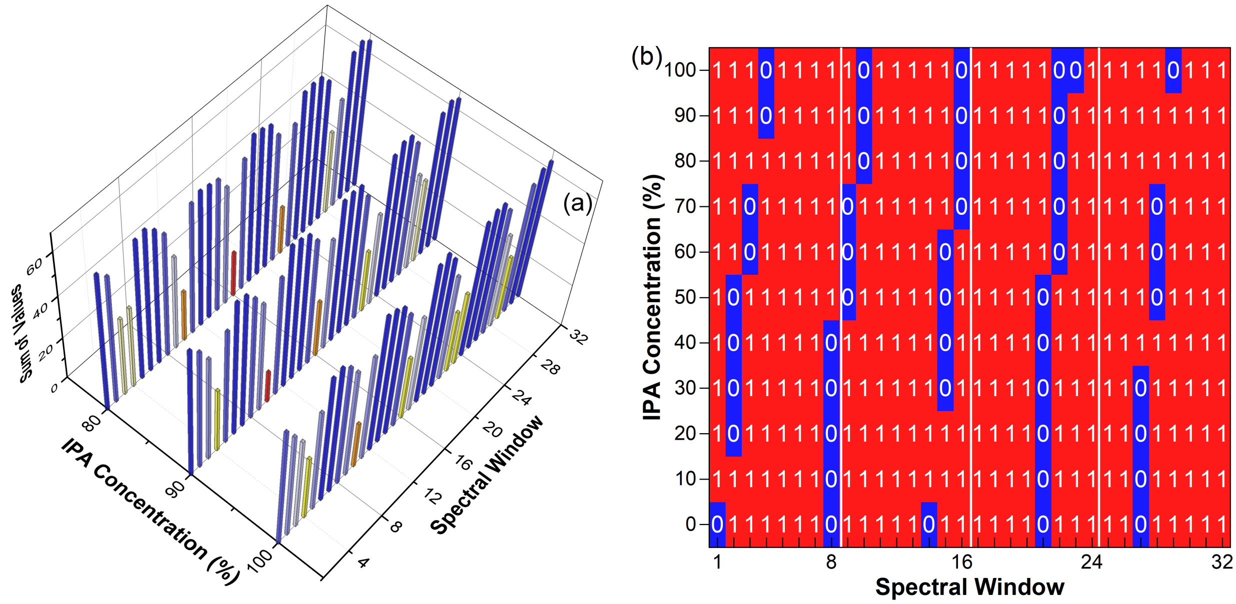

Fig. 6. (a) Histograms of sum of values for IPA concentrations of 80%, 90%, and 100% v/v. These were generated by dividing 5.44 nm of the TFBG transmission spectrum into 32 spectral windows each with a width of 170 pm and by adding the transmission values in each window. (b) Binary codes obtained from (a) when the threshold was set to 36.

and photodetector interrogation systems, we added all the transmitted power values, T_i, over the wavelength in each window, as depicted in Fig. 5. This must be performed for each value of IPA concentration. In this manner, we could calculate a "sum of values" value in each spectral window. As before, an arbitrarily threshold must be set to discretize the results of each window into 0 and 1.

In our case, we analyzed the spectral range from 1564 to 1569.44 nm and set 32 spectral windows; the width of each window was set to 170 pm (typical resolution of a low-cost spectrometer or a multiplexer). We calculated the sum of values for concentrations of IPA from 0% to 100% v/v. The sum of values for the cases of IPA concentrations of 80%, 90%, and 100% v/v are shown in Fig. 6(a). The threshold we used was 36 a.u. in "sum of values." Thus, the values bigger than 36 were set as 1, and those smaller than 36 were set as 0. The binary codes that were obtained with this procedure are shown in Fig. 6(b). Note that in all IPA concentrations, the series of bits are different.

The results shown in Fig. 6 suggest that with a low-cost interrogation system and through discretization of the TFBG spectra, it seems possible to train (machine learning) a sensing device to have standardized bits coming out of TFBG measurements. More importantly, the data size or computer memory needed to encode or decode the IPA concentrations is minimal (2 or 4 bytes only). Such data size can be processed at high speed.

To the best of our knowledge, this is the first time that the discretization of TFBGs spectra has been proposed. Such discretization allows to generate unique set of bits that is the language of digital devices. The set of bits can also be used to generate simple visual labels, such as 1-D barcodes. A potential application of the set of bits or barcodes can be the detection of a concentration threshold. In this case, high spectral resolution may be required but only in a narrow wavelength range and there is no need to track picometer wavelength shifts of narrowband resonances. In addition, no polarizers and polarization controllers may be necessary. These features may reduce substantially the instrumentation necessary to generate barcodes or a set of bits with TFBGs.

Regarding the potential applications of the discretization of TFBG spectral combs, it can be useful, for example, to generate unique identification labels of pure liquids and mixtures. Thus, the applications of TFBGs can be expanded beyond optical sensing.

IV. Conclusion

The output spectra of TFBGs contain abundant data and information about the environment that surrounds the grating. To decode the information contained in the spectrum of a TFBG, multiple techniques have been reported. In most of them, minute changes of amplitude or picometer wavelength shifts of the resonances are tracked. To do so, broadband light sources, high-resolution spectrometers that operate over a wavelength range exceeding 70 nm, and polarization controllers are necessary. The complexity of this interrogation limits the widespread applications of TFBG-based sensors.

As demonstrated here, the spectrum of TFBGs can be analyzed without polarizers, and over a narrow spectral range, high resolution may be necessary but in a small bandwidth. We have demonstrated that IPA concentrations in water can be correlated with a set of bits or with simple 1-D barcodes. The set of bits or barcodes can be used for labeling, coding liquids, or mixtures. Through discretization of the TFBG spectra, sensors can communicate with digital devices or instruments in their language. Therefore, the results shown here may allow us to expand the use of TFBGs beyond optical sensing.

Acknowledgment

The authors are grateful to Luis Villatoro for making the visual shown in Fig. 1.

References

[1] X. Dong, H. Zhang, B. Liu, and Y. Miao, "Tilted fiber Bragg gratings: Principle and sensing applications," *Photonic Sensors*, vol. 1, no. 1, pp. 6–30, Mar. 2011, doi: 10.1007/s13320-010-0016-x.

[2] T. Guo, F. Liu, B.-O. Guan, and J. Albert, "Tilted fiber grating mechanical and biochemical sensors," *Opt. Laser Technol.*, vol. 78, pp. 19–33, Apr. 2016, doi: 10.1016/j.optlastec.2015.10.007.

[3] A. Kameyama, "A simplified fabrication technique for tilted fiber Bragg grating for the simultaneous measurement of refractive index and temperature of liquids," *J. Laser Micro/Nanoeng.*, vol. 9, no. 3, pp. 230–233, Nov. 2014, doi: 10.2961/jlmn.2014.03.0009.

[4] J. Albert, L.-Y. Shao, and C. Caucheteur, "Tilted fiber Bragg grating sensors," *Laser Photon. Rev.*, vol. 7, no. 1, pp. 83–108, Jan. 2013, doi: 10.1002/lpor.201100039.

[5] M. Z. Alam and J. Albert, "Selective excitation of radially and azimuthally polarized optical fiber cladding modes," *J. Lightw. Technol.*, vol. 31, no. 19, pp. 3167–3175, Oct. 1, 2013, doi: 10.1109/JLT.2013.2280581.

[6] A. Ioannou, A. Theodosiou, K. Kalli, and C. Caucheteur, "Higher-order cladding mode excitation of femtosecond-laser-inscribed tilted FBGs," *Opt. Lett.*, vol. 43, no. 9, p. 2169, May 2018, doi: 10.1364/ol.43.002169.

[7] D. Harasim, "Temperature-insensitive bending measurement method using optical fiber sensors," *Sens. Actuators A, Phys.*, vol. 332, Dec. 2021, Art. no. 113207, doi: 10.1016/j.sna.2021.113207.

[8] C. Caucheteur, T. Guo, and J. Albert, "Polarization-assisted fiber Bragg grating sensors: Tutorial and review," *J. Lightw. Technol.*, vol. 35, no. 16, pp. 3311–3322, Aug. 27, 2017, doi: 10.1109/JLT.2016.2585738.

[9] D. Harasim, "Polarization-insensitive refractive index measurement using cascaded perpendicular tilted fiber Bragg gratings," *Measurement*, vol. 202, Oct. 2022, Art. no. 111845, doi: 10.1016/j.measurement.2022.111845.

[10] C. Caucheteur, J. Villatoro, F. Liu, M. Loyez, T. Guo, and J. Albert, "Mode-division and spatial-division optical fiber sensors," *Adv. Opt. Photon.*, vol. 14, no. 1, p. 1, Mar. 2022, doi: 10.1364/aop.444261.

[11] J.-M. Renoirt, C. Zhang, M. Debliquy, M.-G. Olivier, P. Mégret, and C. Caucheteur, "High-refractive-index transparent coatings enhance the optical fiber cladding modes refractometric sensitivity," *Opt. Exp.*, vol. 21, no. 23, Nov. 2013, Art. no. 29073, doi: 10.1364/oe.21.029073.

[12] W. Zhou, D. J. Mandia, S. T. Barry, and J. Albert, "Absolute near-infrared refractometry with a calibrated tilted fiber Bragg grating," *Opt. Lett.*, vol. 40, no. 8, p. 1713, Apr. 2015, doi: 10.1364/ol.40.001713.

[13] W. Zhou, Y. Zhou, and J. Albert, "A true fiber optic refractometer," *Laser Photon. Rev.*, vol. 11, no. 1, Jan. 2017, Art. no. 1600157, doi: 10.1002/lpor.201600157.

[14] S. Cieszczyk, D. Harasim, and P. Kisala, "A novel simple TFBG spectrum demodulation method for RI quantification," *IEEE Photon. Technol. Lett.*, vol. 29, no. 24, pp. 2264–2267, Dec. 15, 2017, doi: 10.1109/LPT.2017.2768601.

[15] Y. Sun, X. Guo, Y. Moreno, Q. Sun, Z. Yan, and L. Zhang, "Sensitivity adjustable biosensor based on graphene oxide coated excessively tilted fiber grating," *Sens. Actuators B, Chem.*, vol. 351, Jan. 2022, Art. no. 130832, doi: 10.1016/j.snb.2021.130832.

[16] B. Jiang and J. Zhao, "Nanomaterial-functionalized tilted fiber gratings for optical modulation and sensing," *J. Lightw. Technol.*, vol. 41, no. 13, pp. 4103–4113, Jul. 1, 2023, doi: 10.1109/JLT.2022.3216728.

[17] K. Tomyshev, E. I. Dolzhenko, A. D. Vasilyeva, L. V. Yurina, and O. V. Butov, "Selective fiber optic TFBG-assisted biosensors featuring functional coatings," *Sens. Actuators B, Chem.*, vol. 384, Jun. 2023, Art. no. 133618, doi: 10.1016/j.snb.2023.133618.

[18] H. Jean-Ruel and J. Albert, "Recent advances and current trends in optical fiber biosensors based on tilted fiber Bragg gratings," *TrAC Trends Anal. Chem.*, vol. 174, May 2024, Art. no. 117663, doi: 10.1016/j.trac.2024.117663.

[19] G. Laffont and P. Ferdinand, "Tilted short-period fibre-Bragg-grating-induced coupling to cladding modes for accurate refractometry," *Meas. Sci. Technol.*, vol. 12, no. 7, p. 765, 2001, doi: 10.1088/0957-0233/12/7/302.

[20] C. Caucheteur and P. Megret, "Demodulation technique for weakly tilted fiber Bragg grating refractometer," *IEEE Photon. Technol. Lett.*, vol. 17, no. 12, pp. 2703–2705, Dec. 2005, doi: 10.1109/LPT.2005.859411.

[21] B. Jiang et al., "Carbon nanotube-deposited tilted fiber Bragg grating for refractive index and temperature sensing," *IEEE Photon. Technol. Lett.*, vol. 28, no. 9, pp. 994–997, May 1, 2016, doi: 10.1109/LPT.2016.2522512.

[22] C.-F. Chan, C. Chen, A. Jafari, A. Laronche, D. J. Thomson, and J. Albert, "Optical fiber refractometer using narrowband cladding-mode resonance shifts," *Appl. Optics*, vol. 46, no. 7, pp. 1142–1149, 2007, doi: 10.1364/AO.46.001142.

[23] Q. Jiang, D. Hu, and M. Yang, "Simultaneous measurement of liquid level and surrounding refractive index using tilted fiber Bragg grating," *Sens. Actuators A, Phys.*, vol. 170, nos. 1–2, pp. 62–65, Nov. 2011, doi: 10.1016/j.sna.2011.06.001.

[24] S.-I. Takeda, M. Sato, and T. Ogasawara, "Simultaneous measurement of strain and temperature using a tilted fiber Bragg grating," *Sens. Actuators A, Phys.*, vol. 335, Mar. 2022, Art. no. 113346, doi: 10.1016/j.sna.2021.113346.

[25] X. Han et al., "In situ surface turbidity sensor based on localized light scattering from tilted fiber Bragg gratings," *Opt. Lett.*, vol. 49, no. 3, p. 650, Feb. 2024, doi: 10.1364/ol.512335.

[26] F. Liu et al., "Detangling electrolyte chemical dynamics in lithium sulfur batteries by operando monitoring with optical resonance combs," *Nature Commun.*, vol. 14, no. 1, p. 7350, Nov. 2023, doi: 10.1038/s41467-023-43110-8.

[27] S. Cai, Y.-G. Nan, Y. Li, Y. Hou, and Z. Zhang, "Rapid detection of hydrogen using narrow bandwidth fiber-optic spectral combs with a low limit of detection," *Opt. Exp.*, vol. 31, no. 22, p. 35616, Oct. 2023, doi: 10.1364/oe.502915.

[28] Y. Singh, S. K. Raghuwanshi, O. Prakash, and P. K. Saini, "Design and development of tilted fiber Bragg grating (TFBG) chemical sensor with regression analysis of grating parameters for sensitivity optimization," *Opt. Quantum Electron.*, vol. 53, no. 11, pp. 1–14, Nov. 2021, doi: 10.1007/s11082-021-03328-6.

[29] B. Jiang, K. Zhou, C. Wang, Y. Zhao, J. Zhao, and L. Zhang, "Temperature-calibrated high-precision refractometer using a tilted fiber Bragg grating," *Opt. Exp.*, vol. 25, no. 21, pp. 25910–25918, Oct. 2017, doi: 10.1364/oe.25.025910.

[30] F. Liu et al., "High-sensitive and temperature-self-calibrated tilted fiber grating biological sensing probe," *Chin. Sci. Bull.*, vol. 58, no. 21, pp. 2611–2615, Jul. 2013, doi: 10.1007/s11434-013-5724-3.

[31] Z. Cao et al., "Improved spectral interrogation of tilted fiber Bragg grating refractometer using residual convolutional neural networks," *J. Lightw. Technol.*, vol. 40, no. 22, pp. 7403–7411, Nov. 15, 2022, doi: 10.1109/JLT.2022.3200999.

[32] Z. Li, F. Wang, Y. Wang, X. Jin, Y. Duan, and H. Zhu, "Decoupling bulk and surface characteristics with a bare tilted fiber Bragg grating," *Opt. Exp.*, vol. 31, no. 12, pp. 20150–20159, Jun. 2023, doi: 10.1364/oe.492110.

[33] Z. X. Huang et al., "Improving accuracy and sensitivity of a tilted fiber Bragg grating refractometer using cladding mode envelope derivative," *J. Lightw. Technol.*, vol. 41, no. 13, pp. 4123–4129, Jul. 1, 2023, doi: 10.1109/JLT.2022.3178268.

[34] D. Okada et al., "Optical microresonator arrays of fluorescence-switchable diarylethenes with unreplicable spectral fingerprints," *Mater. Horizons*, vol. 7, no. 7, pp. 1801–1808, Jul. 2020, doi: 10.1039/d0mh00566e.

[35] J. Liao and L. Yang, "Optical whispering-gallery mode barcodes for high-precision and wide-range temperature measurements," *Light, Sci. Appl.*, vol. 10, no. 1, p. 32, Feb. 2021, doi: 10.1038/s41377-021-00472-2.

[36] X. Zeng, Y. Dong, Y. Li, J. Wang, P. Sun, and H. Wang, "Photonic barcodes based on a SNAP microcavity for displacement sensing," *IEEE Sensors J.*, vol. 22, no. 18, pp. 17830–17837, Sep. 2022, doi: 10.1109/JSEN.2022.3194625.

[37] N. Toropov and F. Vollmer, "Whispering-gallery microlasers for cell tagging and barcoding: The prospects for in vivo biosensing," *Light, Sci. Appl.*, vol. 10, no. 1, p. 77, Apr. 2021, doi: 10.1038/s41377-021-00517-6.

[38] Y. Liu, J. You, and X. Li, "Vacuum pressure imaging solution based on fiber-optic Fabry–Pérot interferometer and optical barcode," *Measurement*, vol. 219, Sep. 2023, Art. no. 113226, doi: 10.1016/j.measurement.2023.113226.

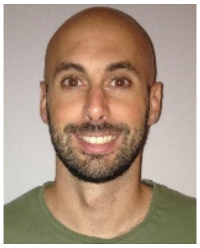

Ander Zornoza received the master's degree in communication technologies, the Ph.D. degree in telecommunication engineering, and the Ph.D. degree in communication technologies from the Public University of Navarre (UPNA), Pamplona, Spain, in 2000, 2008, and 2014, respectively, and the master's degree in civil engineering from the University of Illinois at Chicago, Chicago, IL, USA, in 2024, through the Fulbright Scholarshi

He is currently with the Department of Applied Mathematics, University of the Basque Country UPV/EHU, Bilbao, Spain, as an Associate Professor. He has wide expertise in optical fiber sensors, embedding of fiber optic sensors in metals, and data processing. He has also experience in the fabrication and characterization of photonic devices and an interest in device modeling and simulation and in new sensor signal processing techniques.

Efraín Villatoro (Member, IEEE) received the bachelor's degree in industrial engineering from the National Technology of Mexico (TecNM), Comitán, México, in 2014, and the master's degree in biomedical technology from the National Institute of Astrophysics, Optics, and Electronics (INAOE), Puebla, Mexico, in 2019, where he is currently pursuing the Ph.D. degree in optics science.

His research interests are primarily centered on new kinds of fiber sensors, particularly in fiber Bragg gratings (FBG's) and tilted-FBG devices, for different applications, including plasmonic technologies for biomedical and industrial use.

Plácido Zaca-Morán received the master's degree in electronics and telecommunications from the Centro de Investigación Científica y de Educación Superior de Ensenada (CICESE), Ensenada, Mexico, in 2000, and the Ph.D. degree in optical sciences with a specialization in optical fibers from the Instituto Nacional de Astrofísica, Óptica y Electrónica (INAOE), Puebla, Mexico, in 2006.

He is currently a full-time Research Professor with the Instituto de Ciencias of the Benemérita Universidad Autónoma de Puebla (BUAP), Puebla. He has published over 40 articles in indexed journals and holds several patents related to optical, medical, and biological applications. His research focuses on optical fiber lasers, nonlinear optics, and the development of devices based on nanomaterials for biomedical applications.

Celia L. Gomez received the master's degree in science with a specialization in materials science from the Benemérita Universidad Autónoma de Puebla (BUAP), Puebla, Mexico, in 2010, and the Ph.D. degree in materials science and engineering from the Universidad Nacional Autónoma de México (UNAM), Mexico City, Mexico, in 2016.

She is currently with the Post-Doctoral position funded by CONACYT at the Instituto de Ciencias, BUAP. She actively participates as a professor at higher education institutions and collaborates on various research projects. She has published scientific articles in high-impact international journals related to these research areas. Her research focuses on characterizing nanostructured materials using spectroscopic techniques, such as Fourier transform infrared, Raman, UV–Vis, and electrochemical impedance spectroscopy, and their biomedical applications as electrooptic and biosensors.

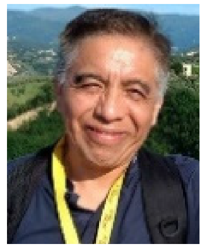

Rubén Ramos-García received the bachelor's degree in physics from the Higher School of Physics and Mathematics (ESFM), National Polytechnic Institute (IPN), Ciudad de Mexico, Mexico, the master's degree from the Center for Research in Optics (CIO), León, Mexico, and the Ph.D. degree from Imperial College London, London, U.K.

He is a Senior Researcher with the Department of Optics, National Institute of Astrophysics, Optics, and Electronics (INAOE), Puebla, Mexico, where he is the Leader of the Biophotonics Group. His areas of research include optical tweezers, optical cavitation, and biophotonics in general.

Dr. Ramos-García is a member of Mexican Academy of Sciences and an Associate Professor at The Abdus Salam International Centre for Theoretical Physics, Trieste, Italy.

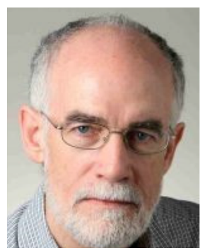

Jacques Albert received the B.Sc. degree in physics from the Universit de Montréal, Montreal, QC, Canada, in 1978, the M.Sc. degree in physics (optics) from Universit Laval, Québec, QC, Canada, in 1980, and the Ph.D. degree in electrical engineering from McGill University, Montreal, in 1988.

He has authored over 150 journal articles in photonics and has several patents. In addition to participation in numerous technical program committees of international conferences, he has cochaired the 2011 Optical Fiber Sensors Conference, and the Topical Meeting on Bragg Gratings, Photosensitivity, and Poling from 2003 to 2007. He currently holds the Canada Research Chair in Advanced Photonic Components with Carleton University, Ottawa, ON, Canada.

Joel Villatoro (Senior Member, IEEE) received the M.Sc. and Ph.D. degrees in optics from the Instituto Nacional de Astrofísica, Óptica y Electrónica (INAOE), Puebla, Mexico, in 1995 and 1999, respectively.

He is currently Ikerbasque Research Professor with the Faculty of Engineering of Bilbao, University of the Basque Country UPV/EHU, Bilbao, Spain. He has nine international patents and more than 93 journal articles and 74 conference papers to his credit. His research interests include the development of advanced plasmonic and interferometric sensors based on conventional and specialty optical fibers, applications of such sensors in real-life scenarios, and development of optical sensors based on nanomaterials for applications in the biomedical, environment, and energy sectors.

Dr. Villatoro has been a Senior Member of SPIE and a fellow of Optica since 2020.